MOLECULAR AND CELLULAR BIOLOGY, Nov. 2004, p. 9424–9436 Vol. 24, No. 21
0270-7306/04/$08.00+0 DOI: 10.1128/MCB.24.21.9424–9436.2004

The Yaf9 Component of the SWR1 and NuA4 Complexes Is Required for Proper Gene Expression, Histone H4 Acetylation, and Htz1 Replacement near Telomeres†

Haiying Zhang,[1,2]‡ Daniel O. Richardson,[1,2]‡ Douglas N. Roberts,[1,2] Rhea Utley,[3] Hediye Erdjument-Bromage,[4] Paul Tempst,[4] Jacques Côté,[3] and Bradley R. Cairns[1,2]*

Howard Hughes Medical Institute[1] and Department of Oncological Sciences,[2] School of Medicine, University of Utah, Salt Lake City, Utah; Molecular Biology Program, Memorial Sloan-Kettering Cancer Center, New York, New York[4]; and Cancer Research Center, Laval University, Quebec City, Quebec, Canada[3]

Received 12 March 2004/Returned for modification 9 April 2004/Accepted 7 August 2004

Yaf9, Taf14, and Sas5 comprise the YEATS domain family in *Saccharomyces cerevisiae*, which in humans includes proteins involved in acute leukemias. The YEATS domain family is essential, as a *yaf9*Δ *taf14*Δ *sas5*Δ triple mutant is nonviable. We verify that Yaf9 is a stable component of NuA4, an essential histone H4 acetyltransferase complex. Yaf9 is also associated with the SWR1 complex, which deposits the histone H2A variant Htz1. However, the functional contribution of Yaf9 to these complexes has not been determined. Strains lacking *YAF9* are sensitive to DNA-damaging agents, cold, and caffeine, and the YEATS domain is required for full Yaf9 function. NuA4 lacking Yaf9 retains histone acetyltransferase activity in vitro, and Yaf9 does not markedly reduce bulk H4 acetylation levels, suggesting a role for Yaf9 in the targeting or regulation of NuA4. Interestingly, *yaf9*Δ strains display reduced transcription of genes near certain telomeres, and their repression is correlated with reduced H4 acetylation, reduced occupancy by Htz1, and increased occupancy by the silencing protein Sir3. Additionally, the spectra of phenotypes, genes, and telomeres affected in *yaf9*Δ and *htz1*Δ strains are significantly similar, further supporting a role for Yaf9 in Htz1 deposition. Taken together, these data indicate that Yaf9 may function in NuA4 and SWR1 complexes to help antagonize silencing near telomeres.

Chromatin structure is a central regulator of gene expression. Nucleosomes are the basic unit of chromatin structure, consisting of a histone octamer disk around which is wrapped 147 bp of DNA. The amino-terminal tails of the histone proteins are exposed on the surface of the nucleosome and serve as platforms to which additional proteins can bind and influence chromatin structure and transcriptional activity, either positively (to form active euchromatin) or negatively (to form repressive heterochromatin) (24). In *Saccharomyces cerevisiae*, the products of the *SIR2*, *SIR3*, and *SIR4* (silent information regulator) genes can bind to histone tails and form repressive heterochromatin by polymerization down the chromatin template (19, 20, 48).

Sir2/3/4 polymerization is observed at telomeres and at the transcriptionally silent mating type loci (20) and is initiated by their recruitment to these loci by the specific DNA-binding protein Rap1. Histone acetylation is a central regulator of the chromatin state; hyperacetylation is associated with transcriptional activation, and hypoacetylation is associated with repression. Sir2/3/4 complexes prefer to bind to deacetylated tails (7), consistent with the observation that the histone tails of transcriptionally silent telomeres are largely deacetylated (50). Importantly, the Sir2 protein itself is an NAD-dependent histone deacetylase whose activity is essential for Sir2/3/4 spreading (23, 31, 47), suggesting that the deacetylation of neighboring nucleosomes by Sir2 enables Sir3/4 binding and subsequent spreading.

Clearly, the spreading distance must be regulated to ensure that important genes near telomeres are not improperly silenced. In principle, heterochromatin boundaries may be formed through the recruitment of factors that oppose heterochromatin spreading. For example, tRNA genes, which are robustly transcribed by RNA polymerase III, contribute to barrier formation at the silent mating type locus *HMR* (10, 11). In addition, certain subtelomeric regions contain binding sites for the transcription factors Reb1 and Tbf1, which help block the spreading of silencing (16, 17). As Sir proteins bind deacetylated histone tails and as Sir2 itself is a deacetylase, histone acetyltransferases (HATs) could provide a potent barrier to Sir propagation. Support for this proposal emerged from work on the SAS complex, which consists of the HAT Sas2, Sas4, and a third protein, Sas5 (33, 40). Sas5 is related to the human leukemogenic proteins AF9/ENL/Gas41 and to the yeast proteins Anc1/Tfg3/Swp29/Taf30/Taf14 (hereafter referred to as Taf14) and the protein characterized in this work, Yaf9 (40). These proteins all contain a conserved YEATS (Yaf9-ENL-AF9-Taf14-Sas5) domain, the function of which is unknown. Importantly, the HAT component Sas2 functions to prevent the spreading of Sir3 to telomere-proximal genes near

* Corresponding author. Mailing address: Department of Oncological Sciences, School of Medicine, University of Utah, 2000 Circle of Hope, Salt Lake City, UT 84112. Phone: (801) 585-1822. Fax: (801) 585-6410. E-mail: brad.cairns@hci.utah.edu.

‡ H.Z. and D.O.R. contributed equally to this work.

† Supplemental material for this article may be found at http://mcb.asm.org/.

the right end of chromosome VI (26, 49), although the role of the YEATS protein Sas5 in this process has not been determined. Sas2 acetylates lysine 16 on the histone H4 tail (H4K16 acetylation) (51), and the Sir2/3/4 complex binds poorly to H4 tails bearing this modification (7), providing one mechanism for the prevention of spreading. Consistent with these results, a K16R replacement in the histone H4 tail promotes Sir complex spreading at certain telomeres (49). Acetylation of histone H3 may also affect spreading, as the severe H3 hypoacetylation observed in *elp3*Δ *gcn5*Δ double mutants causes spreading at telomere 6R (28). In addition, the tethering of diverse HAT components (including SAS and NuA4 complex components) can block Sir spreading at silent mating type loci, further suggesting a role for HAT recruitment in antagonizing silencing (39).

Recently, a central role for the histone H2A variant Htz1 in preventing spreading was demonstrated, as Htz1 is present at certain telomeres and at the silent locus *HMR* and as the loss of Htz1 results in the spreading of Sir proteins at *HMR* and at a subset of telomeres (9, 29, 34). Importantly, the replacement of Htz1 for canonical H2A is an active ATP-dependent process performed by the SWR1 chromatin remodeling complex, and mutations in SWR1 components cause the repression of telomere-proximal genes (27, 35). Certain components of the SWR1 complex are also present in NuA4, raising the possibility that histone acetylation and Htz1 replacement may be coordinated to affect boundary formation. Consistent with this idea, the double-bromodomain protein Bdf1, which binds to acetylated H4 tails, interacts with SWR1 and has a role in establishing the heterochromatin boundary (27, 29, 30). Thus, diverse factors collaborate for boundary formation, and understanding their coordinated functions is an important current area of study.

Our interest in Yaf9 arose from the identification of a related factor, Taf14, as a member of transcription- and chromatin-regulating complexes, including SWI/SNF, TFIID, TFIIF, and NuA3 (6, 21, 25, 41). Together, these results strongly suggest that YEATS proteins are involved in transcription and chromatin structure, but their mechanistic role is not known. In addition, members of the YEATS protein family have an intriguing link to cancer, as they are common translocation partners of the human trithorax (HRX/MLL/ALL-1) gene, forming fusion proteins that cause acute leukemias (37, 52). Recently, Yaf9 was linked to the SWR1 and NuA4 complexes (27, 29, 32, 35). The NuA4 complex is a multiprotein complex that helps regulate ribosomal protein genes (2, 43) as well as *PHO5* (38). The NuA4 component Esa1 is an essential histone H4 HAT (8, 46), and mutations that reduce HAT activity reduce target gene transcription (14, 18). NuA4 also contains approximately eight other proteins that appear to assist in either targeting or regulation and likely correspond to the p400/TIP60 HAT-DNA repair complex in human cells (5, 13, 22).

Here we provide a functional analysis of Yaf9 and show that it is important for proper DNA repair and metabolism and for the acetylation and expression of telomere-proximal genes. We also provide evidence for Yaf9 function in SWR1 complex and Htz1 functions, as *yaf9*Δ mutants are defective in Htz1 deposition at telomere-proximal genes and show extensive overlap with *htz1*Δ mutants in their transcriptional profiles and phenotypes. Additional genetic and genomic work with Yaf9, Taf14, and Sas5 reveals the importance of the YEATS domain and the YEATS protein family to yeast viability and proper gene expression through transcription and chromatin structure.

MATERIALS AND METHODS

Media, genetic methods, and yeast strains. Preparation of media, genetic methods, and strain isolation followed standard procedures. Strain genotypes are shown in Table 1. All gene deletions and epitope tagging were verified by PCR and/or immunoblot analysis; details are available on request.

Plasmids. The *YAF9* gene was isolated from YBC605 genomic DNA by PCR and cloned into plasmid pRS316 (*CEN6 URA3*), and the sequence was verified. Plasmid p416.*MET25* (36) was used to construct plasmids directing the expression of Flag-tagged Yaf9 (pFlag-*YAF9*, pFlag-*yaf9*$_{1–186}$, and pFlag-*yaf9*$_{SDM}$) from the *MET25* promoter. A site-directed mutation of *YAF9* was generated by the Quick Change method (Stratagene). All clones were verified by sequencing; detailed construction information is available on request.

Tandem affinity purification (TAP) of the NuA4 complex. The NuA4 complex was purified from YBC1093 as follows. Eighteen liters of culture was grown to an optical density at 600 nm (OD_{600}) of 9.0 in 2× yeast extract-peptone-dextrose (YPD), and cells were harvested by centrifugation and washed with 0.5× phosphate-buffered saline–5% glycerol. About 320 g of the cell pellet was resuspended in 160 ml of 3× lysis buffer (150 mM HEPES-OH [pH 7.5], 750 mM potassium acetate [pH 7.5], 60% glycerol, 30 mM EDTA, 1.5 mM dithiothreitol [DTT], protease inhibitor [PI] cocktail [2 μg of chymostatin/ml, 2 μM pepstatin A, 0.6 μM leupeptin, 2 mM benzamidine, 1 mM phenylmethylsulfonyl fluoride]). Cell breakage and protein recovery were carried out as described by Sayre et al. (45). The supernatant (310 ml) was augmented with 15.5 ml (1/20 volume) of 3 M potassium acetate and 10.16 g of ammonium sulfate (to 250 mM). After the mixture was stirred for 30 min, 4.65 ml (1/66.7 volume) of 10% (vol/vol) polyethylenimine (pH 8.0) was added. The mixture was stirred for 10 min and spun in a Beckman 45Ti rotor at 45,000 rpm for 2 h. The supernatant was recovered and supplemented to 0.1% NP-40 with stirring.

NuA4 was purified as described by Puig et al. (42) with the following modifications. A whole-cell extract (297.5 ml at 29 mg/ml) was used directly for immunoglobulin G (IgG) binding; IgG beads were washed four times with wash buffer supplemented with 400 mM NaCl, 0.5 mM DTT, and PIs and washed three times with tobacco etch virus protease (TEV) cleavage buffer. TEV cleavage was performed for 3 h at 15°C; calmodulin binding was performed for 2 h at 4°C. Calmodulin-bound proteins were eluted with supplemented calmodulin elution buffer (25 mM Tris-HCl [pH 7.5], 500 mM NaCl, 1 mM imidazole, 4 mM EGTA, 10% glycerol, 0.1% NP-40, 1 mM DTT, PIs). The calmodulin elution fractions were analyzed by sodium dodecyl sulfate (SDS)-polyacrylamide gel electrophoresis (PAGE) followed by silver staining and Western analysis. Peak fractions were pooled, and about 4.4 ml of final purified NuA4 product (at an estimated concentration of 20 μg/ml) was obtained. Details regarding the purification of hemagglutinin (HA) epitope-tagged Yaf9 and protein identification of NuA4 complex members are in the supplemental data.

HAT assays. Reaction mixtures (40 μl) contained free recombinant yeast core histones (800 ng), 2 μl (~40 ng) of purified NuA4 complex (or buffer as a control), and 0.1 μCi of ^{3}H-acetyl coenzyme A (3.8 Ci/mmol; Sigma) in HAT buffer (50 mM Tris-HCl [pH 8], 50 mM NaCl, 0.1 mM EDTA, 1 mM $MgCl_2$, 25 μg of bovine serum albumin/ml, 1 mM DTT) and were incubated at 30°C for 30 min. Samples were processed essentially as described previously (2). The reaction mixtures were separated on an SDS–10 to 20% gradient acrylamide gel, followed by Coomassie blue staining, destaining, and fluorography with Amplify (Amersham).

RNA preparation and microarray analysis. Relevant strains were grown in YPD at 30°C to an OD_{600} of 0.8. Cells were collected and frozen in liquid nitrogen. Total RNA was isolated by acid phenol-chloroform extraction. Total RNA was treated with RNase-free DNase I and purified with a Qiagen RNeasy kit. Antisense RNA (aRNA) was amplified with an Arcturus RiboAmp RNA amplification kit. aRNA (2 μg) was subjected to microarray analysis as described by Angus-Hill et al. (3). Cy3 and Cy5 fluorescence readings were quantified and normalized such that the average Cy5/Cy3 intensity ratio was equal to 1. All experiments were performed in triplicate, and the $\log_2$ average ratios are reported. Significantly affected genes in the mutants were identified by a change in expression of twofold or more compared to the expression in the relevant wild-type (WT) strains.

ChIP. Sir3 was tagged at its C terminus with 13 copies of the Myc epitope (Myc_{13}) and Htz1 was tagged at its N terminus with 3 copies of the HA epitope

TABLE 1. Strains used in this study[a]

Strain	Genotype	Source or reference
YBC605	*MAT***a** *his3Δ200 leu2Δ0 met15Δ0 trp1Δ63 ura3Δ0*	This work
YBC608	*MATα leu2Δ0 lys2Δ0 ura3Δ0*	This work
YBC785	*MAT***a** *his4-912Δ leu2Δ1 lys2-128Δ ura3-52 tfg3Δ::LEU2*	G. Hartzog
YBC925	*MAT***a** *ade2Δ::hisG his3Δ200 leu2Δ0 lys2Δ0 met15Δ0 trp1Δ63 ura3Δ0 YAF9::His_7-HA_3::TRP1*	This work
YBC1041	*MATα his3Δ1 leu2Δ0 lys2Δ0 ura3Δ0 swr1Δ::KanMX*	Research Genetics
YBC1093	*MATα his3Δ leu2Δ0 lys2Δ0 trp1Δ63 ura3Δ0 YAF9::TAP::TRP1 pep4Δ::KanMX*	This work
YBC1150	*MATα his3Δ1 leu2Δ0 lys2Δ0 ura3Δ0 sas5Δ::KanMX*	Research Genetics
YBC1582	*MATα ade2Δ::hisG his3Δ200 leu2Δ0 lys2Δ0 met15Δ0 trp1Δ63 ura3Δ0 yaf9Δ::HIS3*	This work
YBC1644	*MAT***a** *his3Δ200 leu2-3,112 trp1Δ1 ura3-52 esalΔ::HIS3 esal-L327S::URA3*	8
YBC1646	*MAT***a** *his3Δ200 leu2-3,112 trp1Δ1 ura3-52 esalΔ::HIS3 esal-L254P::URA3*	8
YBC1648	*MAT***a** *his3Δ200 leu2-3,112 trp1Δ1 ura3-52 esalΔ::HIS3* (*esal-Δ414/TRP1/CEN*)	8
YBC1665	*MATα ade2Δ::hisG his3Δ200 leu2Δ0 lys2Δ0 met15Δ0 trp1Δ63 ura3Δ0*	This work
YBC1681	*MAT***a** *his3Δ200 leu2-3,112 trp1Δ1 ura3-52 EP11::TAP::TRP1*	J. Cote
YBC1682	*MAT***a** *his3Δ200 leu2-3,112 trp1Δ1 ura3-52 EP11::TAP::TRP1 yaf9Δ::KanMX*	J. Cote
YBC1740	*MATα lys2-128Δ leu2Δ1 ura3-52 trp1Δ63 his3Δ200 pep4Δ::KanMX yaf9$_{1-186}$::TAP::TRP1*	This work
YBC1741	*MATα ade2Δ::hisG his3Δ200 leu2Δ0 lys2Δ0 met15Δ0 trp1Δ63 ura3Δ0 yaf9Δ::HIS3 SIR3::Myc13::TRP1*	This work
YBC1742	*MATα ade2Δ::hisG his3Δ200 leu2Δ0 lys2Δ0 met15Δ0 trp1Δ63 ura3Δ0 SIR3::Myc13::TRP1*	This work
YBC1825	*MATα ade2Δ::hisG his3Δ200 leu2Δ0 lys2Δ0 met15Δ0 trp1Δ63 ura3Δ0 sir3Δ::KanMX*	This work
YBC1828	*MATα ade2Δ::hisG his3Δ200 leu2Δ0 lys2Δ0 met15Δ0 trp1Δ63 ura3Δ0 yaf9Δ::HIS3 sir3Δ::KanMX*	This work
YBC1864	*MAT***a** *his3Δ1 leu2Δ0 ura3Δ0 met15Δ0 htz1Δ::KanMX*	Research Genetics
YBC1867	*MATα HHT1-HHF1* Δ(*HHT2-HHF2*) *leu2-3,112 ura3-52 lys2Δ201 HA_3-HTZ1*	M. Smith
YBC1895	*MATα his3Δ1 leu2Δ0 lys2Δ0 ura3Δ0*	Research Genetics
YBC1975	*MATα his3Δ1 leu2Δ0 lys2Δ0 ura3Δ0 sas5Δ::KanMX yaf9Δ::HIS3*	This work
YBC1993	*MATα his4-912Δ leu2 lys2 ura3 tfg3Δ::LEU2 sas5Δ::KanMX*	This work
YBC2025	*MATα ade2Δ::hisG his3Δ200 leu2Δ0 lys2Δ0 met15Δ0 trp1Δ63 ura3Δ0 yaf9Δ::HIS3 tfg3Δ::LEU2*	This work
YBC2084	*MATα HHT1-HHF1* Δ(*HHT2-HHF2*) *leu2-3,112 ura3-52 lys2Δ201 HA_3-HTZ1 yaf9Δ::URA3*	This work

[a] All strains are derivatives of the S288C genetic background.

(HA_3) in the WT and *yaf9*Δ backgrounds, respectively. Isogenic untagged strains were used in control experiments. Chromatin immunoprecipitation (ChIP) experiments were performed as described by Roberts et al. (44) with the following modifications. Cells were cross-linked with 1% formaldehyde for 45 min at room temperature. For Sir3-Myc ChIP, 2 μl of anti-Myc antibody (9E11; Abcam) was prebound to 50 μl of pan-mouse IgG Dynabeads (~2.0×10^7 beads; Dynal Biotech catalog no. 110.23) and then incubated with 500 μg (protein) of supernatant from the sheared chromatin for 5 h at 4°C. For HA-Htz1 ChIP, 2 μg of anti-HA antibody (12CA5) and 800 μg of supernatant from the sheared chromatin were incubated overnight at 4°C. For histone H4 tetra-acetylation ChIP, 2 μl of anti-acetylated histone H4 antibody (Upstate Biotechnology catalog no. 06-866) was prebound to 35 μl of sheep anti-rabbit IgG M-280 Dynabeads (~2.0×10^7 beads; Dynal Biotech catalog no. 112.04) and then incubated with 500 μg of protein overnight at 4°C. A total of 6.25 μg of poly(dA)-poly(dT) (Amersham Pharmacia catalog no. 27-7860-02) was used in all ChIP experiments to reduce the nonspecific background. All experimental ChIPs were performed in triplicate, and untagged control ChIPs were performed in duplicate. The purified ChIP samples were used in quantitative PCR (qPCR) analysis and genome-wide ChIP (G-ChIP) analysis.

Real-time qPCR analysis. qPCR was performed as described by Roberts et al. (44), except that all PCRs were performed in triplicate and the average was calculated as the relative abundance of each target of interest. *ACT1*, *ARS317*, and *PRP8* were used as the normalization controls to determine the enrichment of targets in Sir3, acetyl-histone H4, and Htz1 occupancy studies, respectively. Primer sequences are available on request.

RESULTS

Yaf9 and the YEATS domain protein family. Our interest in Yaf9 was based on a previous identification of its paralog, Taf14, as a member of the SWI/SNF complex and also on its sequence similarity to proteins such as AF9 and ENL, which are involved in human leukemias. Searches using the Basic Local Alignment Search Tool (BLAST) algorithm showed that Yaf9 was significantly more similar to AF9 (BLAST E-value of 1e −16) (and also to ENL) than was Taf14 (BLAST E-value of 1e −9); therefore, we named the protein Yaf9 (yeast AF9). However, more recent searches have revealed a much larger family, including proteins in *Schizosaccharomyces pombe* and *Caenorhabditis elegans* and additional human proteins, such as Gas41 (BLAST E-value of 1e −29) (Fig. 1A and B). All members bear a defining N-terminal YEATS domain and therefore have been termed YEATS family members (Fig. 1A). However, close inspection of these protein sequences and analysis by BLAST suggest the presence of three additional sequence elements, which we termed the A, B, and C boxes, that we believe are useful for classifying the members (Fig. 1B). The A box is present in many members but is absent in Taf14 and Sas5. The B box defines the C terminus of Yaf9, Gas41, and related proteins and is predicted to form a coiled coil (Fig. 1B and data not shown). Although the B box is absent in AF9 and ENL, these two proteins share homology at their C termini, and this region is also predicted to form a coiled coil. The C box is present only at the C termini of Taf14 and Sas5. Taken together, these results indicate that the family appears to be comprised of three sequence classes: a Yaf9/Gas41 class (A box, with a B box at the C terminus), an AF9/ENL class (A box, with a coiled coil at the C terminus), and a Sas5/Taf14 class (C box at the C terminus).

The YEATS family is essential in *S. cerevisiae*. To determine the importance of the YEATS family in yeast cells, we isolated strains bearing combinations of null mutations in the three family members (Yaf9, Sas5, and Taf14). Although no individual member was essential, strains lacking two of the three members showed reduced growth ability, and a strain lacking all three was nonviable (Table 2). These results establish the YEATS family as being essential in yeast cells.

Yaf9 is a stable member of the NuA4 complex. Initially, we determined that Yaf9 localizes to the nucleus (Fig. 1C), con-

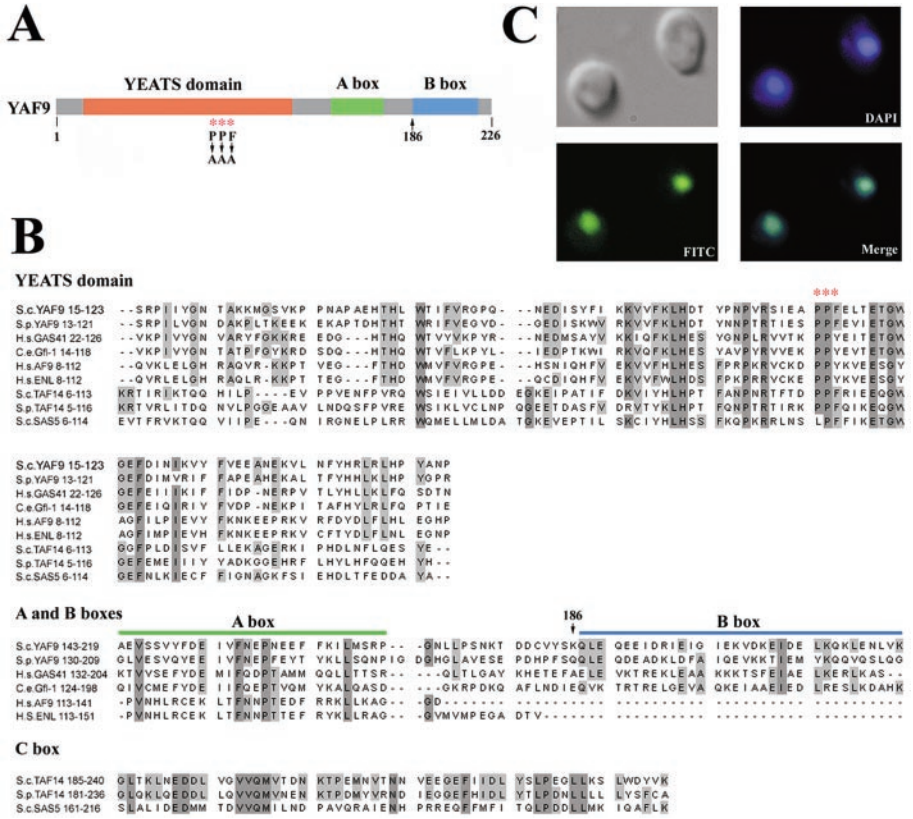

FIG. 1. Yaf9 localization and YEATS domain alignments. (A) Diagram of Yaf9 domain structure. Boxes represent the YEATS domain, the A box, and the B box. Asterisks indicate the positions of site-directed mutations for $yaf9_{SDM}$; the arrow at position 186 indicates the last amino acid present in the C-terminal truncation construct $Yaf9_{1–186}$. (B) Alignments of YEATS domains and three newly identified homology regions, the A box, the B box, and the C box. S.c., *S. cerevisiae*; S.p., *S. pombe*; H.s., *Homo sapiens*; C.e., *C. elegans*. (C) Yaf9 is localized to the nucleus. Immunofluorescence studies were carried out with strain YBC1093, bearing TAP-tagged Yaf9. Images of cells, 4′,6′-diamidino-2-phenylindole (DAPI) staining, and fluorescein isothiocyanate (FITC) staining (with anti-protein A primary antibody) and a merged image of DAPI staining and FITC staining are shown (see the supplemental data).

sistent with a role in transcription. To identify associated proteins, Yaf9 was tagged at the C terminus with one of two different tandem affinity tags. One consisted of a tandem HA_3-His_7 tag, and the other consisted of a tandem protein A–calmodulin-binding protein (TAP) tag (see Materials and Methods). DNA encoding each tag was targeted to the 3′ end of chromosomal *YAF9* by homologous recombination. The tags did not affect function, as strains bearing these tags lacked the

TABLE 2. Growth phenotypes

Relevant genotype	Growth under the following conditions[a]:					
	28°C	15°C	5 mM caffeine	50 mM HU	UV	0.03% MMS
WT (YBC1665)	+	+	+	+	+	+
*yaf9*Δ	+/−	−	−/+[b]	−/+	−	−
*sas5*Δ[c]	+	+	+	+	+	+
*taf14*Δ	−/+ to +/−	+/−	−/+	− to −/+	−	−
*taf14*Δ + pRS316.$taf14_{SDM}$	+/−	+ to ++	−/+	− to −/+	−/+	−
esa1-L254P	+/−	+/− to +	+[b]	+	−/+ to +/−	−
*sas5*Δ *yaf9*Δ	+/−	−	+/−	+/−	− to −/+	−
*taf14*Δ *yaf9*Δ	+/−	−	−/+	+/−	− to −/+	−
*sas5*Δ *taf14*Δ	−/+ to +/−	+/−	+	−	−	−
*esa1-L327S yaf9*Δ	Nonviable					
*yaf9*Δ *taf14*Δ *sas5*Δ	Nonviable					
*swr1*Δ[c]	+	−/+	+[d]	−/+	+	+/−
*htz1*Δ[c]	+/−	−	+/−[b]	−	−[e]	−/+

[a] Scoring: ++, very fast growth; +, WT growth; +/−, slow growth; −/+, very slow growth; −, no growth.
[b] With 15 mM caffeine, the score was −.
[c] Growth was compared to that of YBC1895 (WT).
[d] With 15 mM caffeine, the score was −/+.
[e] As reported by Mizuguchi et al. (35).

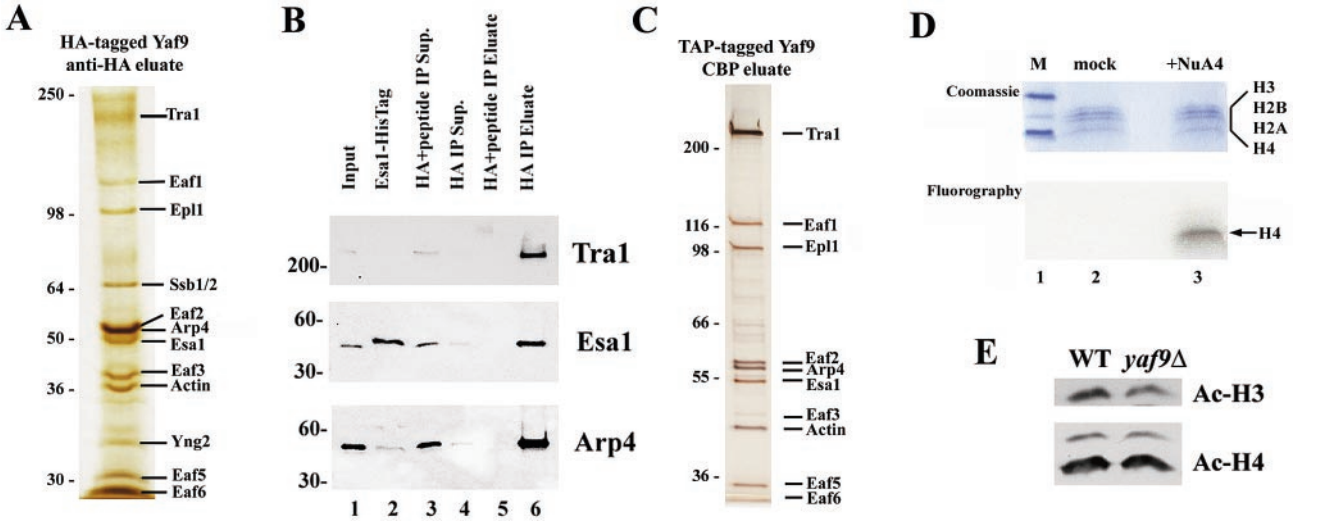

FIG. 2. Yaf9 is a stable component of the NuA4 HAT complex. (A) Purification of HA-tagged Yaf9 yields the NuA4 complex. Extracts were chromatographed on SP Sepharose, DEAE, nitrilotriacetic acid-nickel, Resource Q, and anti-HA–Sepharose columns sequentially (see the supplemental data). The anti-HA eluate was analyzed by SDS-PAGE and silver staining and used for mass spectrometric sequencing (see the supplemental data). Numbers at left are molecular weight markers. (B) Yaf9 is tightly associated with NuA4. Coimmunoprecipitation was carried out with the eluates from Resource Q and anti-HA beads. Immune complexes were washed at a high stringency (400 mM NaCl). Lanes: 1, input (100 μg, 15% of total); 2, His_6-purified recombinant Esa1; 3 and 4, supernatants (Sup.) from immunoprecipitations (IP) in which a competing HA peptide (10 μg) was either included (lane 3) or omitted (lane 4); 5 and 6, elutions with 10% SDS (see the supplemental data). (C) Purification of TAP-tagged Yaf9 yields the NuA4 complex. Twenty microliters of eluate from a calmodulin column (see Materials and Methods) was separated by SDS–7.5% PAGE followed by silver staining. CBP, calmodulin-bound protein. (D) NuA4 bearing Yaf9 displays histone H4 HAT activity. Two microliters of eluate from a calmodulin column was incubated with 800 ng (total) of free recombinant yeast histones as described in Materials and Methods. The reaction mixtures were separated on an SDS–10 to 20% acrylamide gradient gel, followed by Coomassie blue staining (top panel), destaining, treatment with Amplify, and fluorography (bottom panel). M, molecular mass standards (upper band, 16 kDa; lower band, 6 kDa). (E) *yaf9*Δ strains retain WT histone H4 acetylation. WT or *yaf9*Δ whole-cell extracts were probed with either anti-acetyl-lysine 9 or 14 H3 or anti-hyperacetylated H4 antibodies (Upstate). Ac, acetylated.

phenotypes displayed by the null allele (described below). For the strain with the HA_3-His_7 tag, the final anti-HA affinity column afforded nine proteins, which were identified by mass spectrometry to be Eaf1, Eaf2/God1, Eaf3, Eaf5, Eaf6, Epl1, Esa1, Act1, and Nbn1/Yng2, all members of the NuA4 complex.

To assess the stability of the association, we performed coimmunoprecipitation analyses with anti-HA beads and the eluate from the Resource Q column (Fig. 2B). NuA4 members could be depleted from the fraction with anti-HA beads (Fig. 2B, lane 4) and recovered in the eluate (lane 6). Yaf9-NuA4 complexes resisted extensive washing with 400 mM NaCl, showing that Yaf9 is stably associated with NuA4.

The alternative TAP tag procedure enabled the rapid preparation of a pure Yaf9-NuA4 complex (Fig. 2C), which was confirmed by mass spectrometric sequencing and immunoblot analysis (data not shown). TAP-Yaf9 itself stains poorly with silver and migrates at approximately the same mass as Yng2 (36 kDa). However, mass spectrometric analysis of NuA4 prepared by conventional chromatographic methods (18) clearly identified peptides corresponding to Yaf9 (data not shown). Taken together, these data establish Yaf9 as a stable component of NuA4.

NuA4 bearing Yaf9 (purified by the TAP procedure) displayed robust acetyltransferase activity that was highly specific for histone H4 (Fig. 2D). However, activity was essentially equal to that displayed by NuA4 lacking Yaf9 (isolated from a *yaf9*Δ strain bearing Epl1-TAP) (data not shown), suggesting that Yaf9 is not required for HAT activity or for H4 specificity. In addition, SDS-PAGE and Western analysis revealed the presence of all other NuA4 subunits in purified preparations from *yaf9*Δ strains (data not shown), indicating that Yaf9 is not required for complex assembly. Finally, strains lacking *YAF9* showed little or no reduction in their bulk levels of H4 acetylation (Fig. 2E), further suggesting that Yaf9 does not have a great impact on NuA4 H4 HAT activity or that its impact is limited to certain loci (such as telomeres; see below).

Clear evidence for the presence of Yaf9 in the SWR1 complex was recently demonstrated by others (27, 29, 35). Although SWR1 complex members were not clearly detectable by SDS-PAGE analysis in our preparations, components of SWR1 could be detected by immunoblot analysis of preparations from Yaf9 immunoprecipitations performed at a low stringency, and the Ruv helicases could be detected by mass spectrometric analysis at low levels (data not shown). Consistent with stringency affecting the Yaf9-Swr1 association, preparations of the SWR1 complex purified at a low stringency by others contained only substoichiometric amounts of Yaf9, although its presence was definitive. In addition, the placement of a tag on Yaf9 could, in principle, have slightly compromised its association with the SWR1 complex selectively.

Yaf9 is required for proper DNA repair, DNA metabolism, and growth at low temperatures. A strain lacking *YAF9* was viable but was unable to grow at 15°C (Cs^-), on medium containing 0.03% methyl methanesulfonate (MMS; a DNA-damaging agent) or caffeine (5 to 15 mM; elicits a stress re-

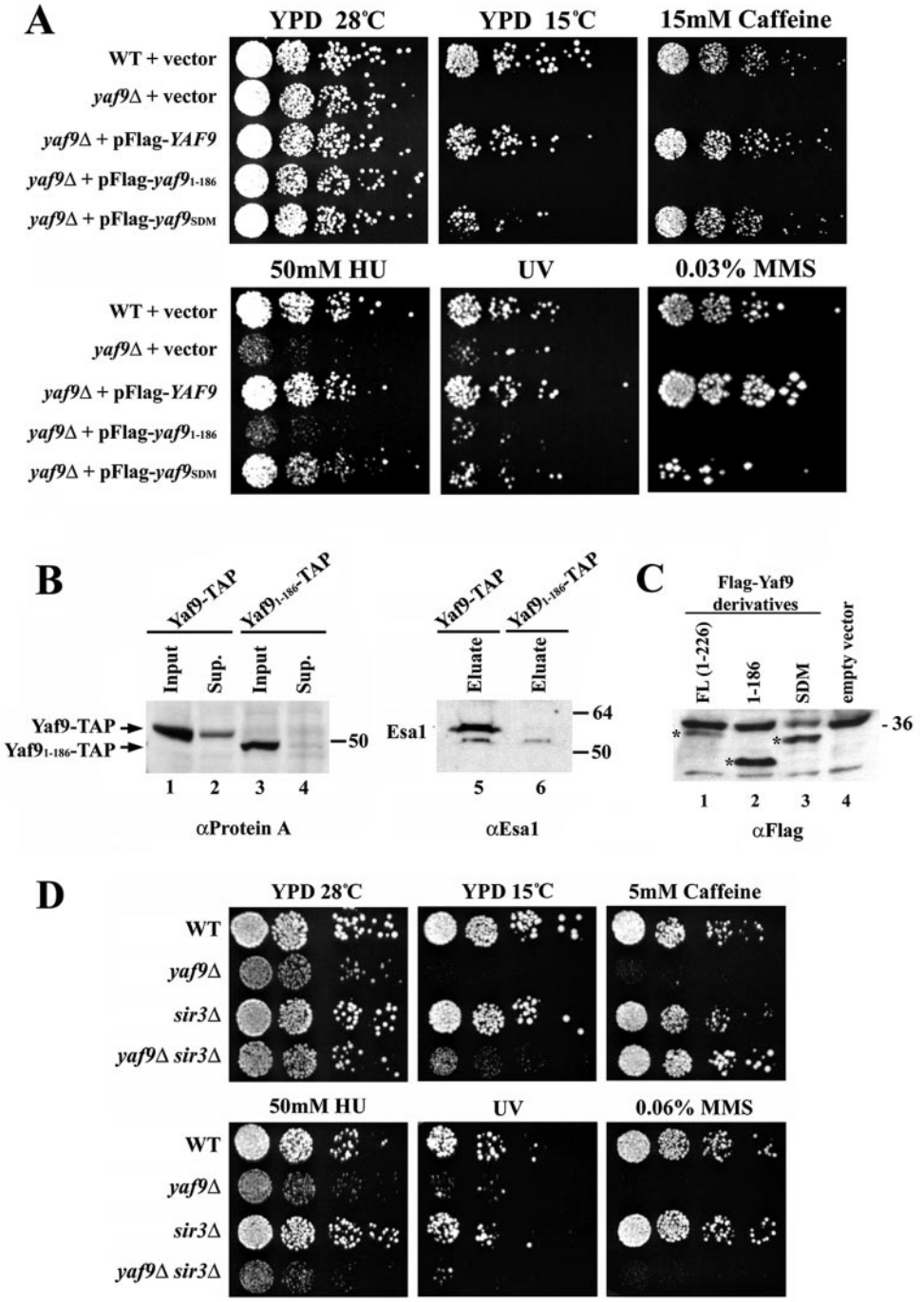

FIG. 3. Structure-function analysis of Yaf9. (A) Phenotypes conferred by *yaf9*Δ and complementation tests with plasmids bearing Yaf9 derivatives. Plasmids used were empty vector pM25, pFlag-*YAF9*, pFlag-$yaf9_{1-186}$, and pFlag-$yaf9_{SDM}$. Strains used were WT YBC1665 and *yaf9*Δ YBC1582. (B) The C terminus of Yaf9 is required for assembly into NuA4. Extracts were prepared from YBC1093 (Yaf9-TAP) and YBC1740 ($Yaf9_{1-186}$-TAP) and loaded into an IgG column. Bound complexes were washed, cleaved with TEV protease, and analyzed by immunoblotting. Equivalent amounts (20 μg) of inputs (lanes 1 and 3) and supernatants (Sup.) (lanes 2 and 4) were loaded side by side and probed with anti-protein A antibody to compare IgG-binding efficiencies. The TEV cleavage eluate from 600 μg of input was probed with anti-Esa1 antibody (lanes 5 and 6) (see the supplemental data). (C) Yaf9 derivatives are stably expressed. Flag-tagged full-length Yaf9 [FL(1-226)], Flag-$yaf9_{1-186}$ (1-186), Flag-$yaf9_{SDM}$ (SDM), or empty vector whole-cell extracts were probed with anti-Flag antibody. Asterisks indicate the Flag-Yaf9 derivatives. (D) Suppression of particular *yaf9*Δ phenotypes by *sir3*Δ. Strains YBC1665 (WT), YBC1582 (*yaf9*Δ), YBC1825 (*sir3*Δ), and YBC1828 (*yaf9*Δ *sir3*Δ) were compared for growth with the indicated media and conditions.

sponse), or after exposure to UV radiation (80 J/m^2) and grew very slowly on 50 mM hydroxyurea (HU; an inhibitor of deoxynucleoside triphosphate synthesis) (Fig. 3A). *nua4* and *swr1* complex mutants share most of these phenotypes (MMS$^-$, caffeine negative, and HU$^-$) (12), making it impossible to attribute these phenotypes in the *yaf9*Δ strain to a function in one particular complex (Table 2). However, we found that *swr1*Δ and *htz1*Δ strains were also Cs$^-$, while NuA4 mutants (*esa1*, *eaf3*Δ, *epl1*, or *arp4*) were not (data not shown), suggesting that Yaf9 promotes growth in the cold through its function exclusively through SWR1/Htz1. Furthermore, we found that *yaf9*Δ *esa1-L327S* double mutants were nonviable (Table 2), with the combination of these two mutations possibly reducing NuA4 function below a critical threshold. Taken together, these results are consistent with functions for Yaf9 in both the SWR1 complex and the NuA4 complex.

Functional requirements for the YEATS and C-terminal domains. The Yaf9 C terminus contains a B box that is predicted to form a coiled coil. The function of this domain is not known, although leukemogenic MLL fusions to YEATS family members all contain their extreme C terminus, suggesting a crucial role for this domain. Deletion of the B box (Yaf9$_{1–186}$) conferred a null phenotype (Fig. 3A), although the derivative was produced well (Fig. 3C). Interestingly, full-length Yaf9 coprecipitated Esa1, whereas Yaf9$_{1–186}$ did not, showing that the Yaf9 C terminus is critical for assembly into NuA4 (Fig. 3B).

A Yaf9 derivative lacking the YEATS domain was unstable and almost undetectable in extracts by immunoblot analysis. Therefore, we prepared a Yaf9 derivative bearing site-directed mutations (SDM) that replaced three consecutive conserved residues in the YEATS domain (PPF, residues 80 to 82) with alanines (Fig. 1A and B). This derivative (Yaf9$_{SDM}$) was stably produced (Fig. 3C) and behaved as a moderate hypomorph; it fully complemented *yaf9*Δ phenotypes related to caffeine and HU sensitivity, partially complemented phenotypes related to cold and UV, but only weakly complemented MMS sensitivity (Fig. 3A). To determine whether the YEATS domain is required for the functions of other YEATS proteins in yeast cells, we created an identical site-directed mutation in Taf14 (termed *taf14*$_{SDM}$) and tested it for complementation of *taf14*Δ phenotypes. We found that the *taf14*Δ mutation conferred sensitivity to temperature (Ts$^-$), caffeine (5 mM), HU (50 mM), UV (80 J/m^2), and MMS (0.03%). Although expressed at WT levels (data not shown), the *taf14*$_{SDM}$ mutation only partially complemented UV and caffeine sensitivity and failed to complement Ts$^-$, MMS$^-$, and HU$^-$ phenotypes (Table 2). Taken together, these results show that the YEATS domain is important for many of the functions of Yaf9 and Taf14, providing the first evidence for a function for the YEATS domain in vivo.

Strains lacking Yaf9 display reduced transcription of genes near certain telomeres and *HMR*. To better understand the impact of Yaf9 on transcription, we compared the transcription profiles for *yaf9*Δ and WT strains. Overall, 224 genes are downregulated more than twofold, whereas 48 genes are upregulated more than twofold. These changes could largely be reversed by transforming the strain with a plasmid bearing WT *YAF9* (data not shown). The majority of the changes observed did not fall into clear gene classes or pathways (the results obtained with the entire microarray are available on request). However, an examination of the changes relative to the physical chromosomal map revealed a striking position effect; a significant fraction of the genes (65 of 224) that were downregulated more than twofold (defined as "affected " genes) in the *yaf9*Δ strain were positioned within 20 kb of the telomere (Fig. 4).

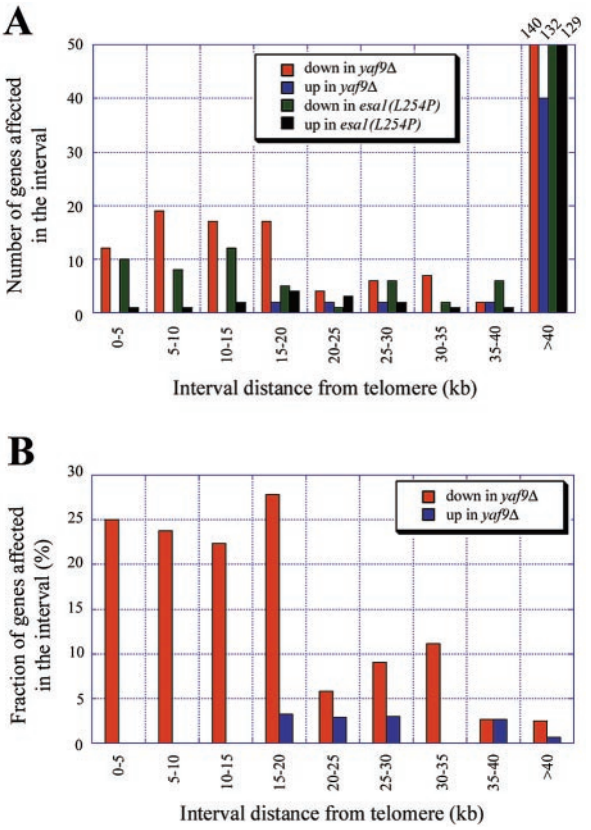

FIG. 4. Genes proximal to telomeres are downregulated in *yaf9*Δ and *esa1-L254P* strains. (A) Numbers of genes downregulated in *yaf9*Δ (red) and *esa1-L254P* (green) strains or upregulated in *yaf9*Δ (blue) and *esa1-L254P* (black) strains (compared to a WT strain) versus their distance from the telomere in 5-kb intervals up to 40 kb. Strains used were *yaf9*Δ YBC1582, *esa1-L254P* YBC1646, WT YBC1665 (for YBC1582), and WT YBC605 (for YBC1646). (B) As in panel A, but with the ordinate showing the fractions of genes downregulated in the interval. Ratios (*yaf9*Δ/WT transcript levels) for each gene from three independent transcription profiling experiments were averaged (see Materials and Methods). Genes that were downregulated >2-fold and located in the interval are represented.

To depict this relationship, we first parsed the 40 kb of DNA proximal to telomeres into eight successive intervals of 5 kb and considered the remainder of the genome (distances of >40 kb) as the final interval (Fig. 4, abscissa). Affected genes were represented on the ordinate in terms of either total number (Fig. 4A) or the fraction of genes affected in the particular interval (Fig. 4B). Although the majority of the genes affected were not within 20 kb of the telomere (Fig. 4A), the density of the affected genes was exceptionally high within 20 kb of the telomere (~25%) compared to the bulk of the genome (~2%). Stated differently, although the telomere-proximal 20-kb region contains only ~5% of all genes, it contains ~29% of the

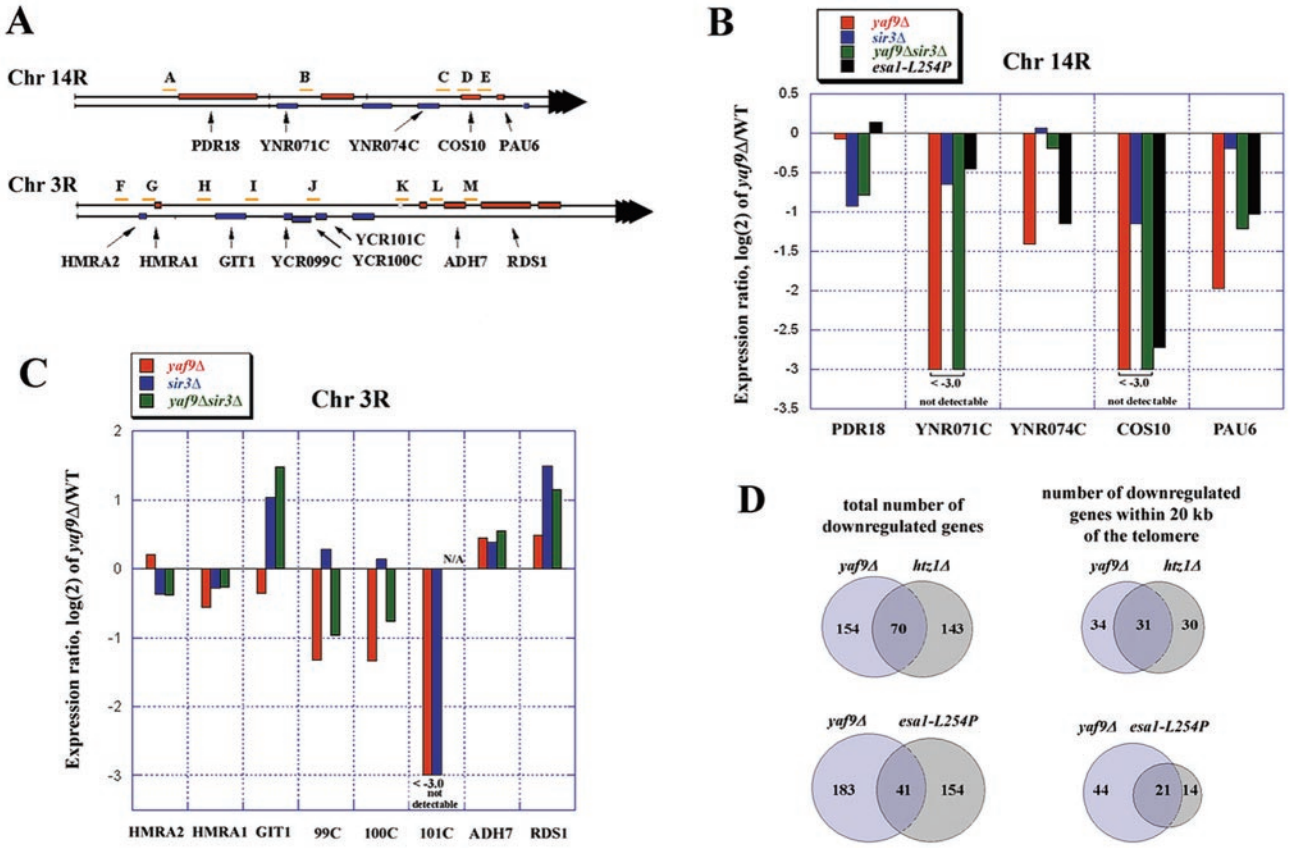

FIG. 5. Transcriptional profiles of *sir3*Δ *yaf9*Δ, *sir3*Δ *yaf9*Δ, and *esa1-L254P* at telomeres 14R and 3R. (A) Physical maps of loci near telomeres 14R (top) and 3R (bottom) with the chromosome (Chr) end at right (black arrowheads). Locations of primer set amplicons used for qPCR are shown above the physical maps in gold. All amplicons were between 239 and 290 bp. (B and C) Genes near telomeres 14R (B) and 3R (C) are strongly downregulated in *yaf9*Δ strains, and certain loci are partially restored by the loss of Sir3. Values are presented as the $\log_2$ ratios for *yaf9*Δ strains compared to WT strains and are the median values of three independent experiments. Loci downregulated >8-fold ($\log_2$ value of −3) fell below the limit of detection. For each of these loci, the spot itself was present and visible on the array, as the Cy3 intensity derived from the WT sample was clearly present; we simply did not observe Cy5 intensity derived from the mutant sample at this locus, the definition of strong downregulation. N/A, not available, as the Cy3 intensity derived from the WT sample fell below the limit of detection in at least one experiment. (D) Venn diagrams depicting the overlap of affected genes (downregulated >2-fold) in the mutants and intervals indicated.

affected genes. This overlap is highly significant; the χ^2 value generated by 65 genes affected within 20 kb of a telomere is 184.9, corresponding to a P value of <0.001. Affected genes were not lost from the telomere due to shortening; genomic DNA isolated from *yaf9*Δ strains was labeled and hybridized to the array and revealed no loss of telomere-proximal genes (data not shown).

Extensive overlap of affected telomeres and genes in *htz1*Δ and *yaf9*Δ strains. Interestingly, only a subset of telomeres is affected in *yaf9*Δ strains. We define affected telomeres as those bearing within 20 kb three or more genes that are downregulated more than twofold. Certain telomeres are highly homologous to telomeres on other chromosomes. For this subset, it is difficult to attribute the downregulation of a transcript observed to gene silencing at a particular gene or telomere, as the transcript (labeled cDNA) derived from one telomere will hybridize to the spot on the microarray representing both homologs. Therefore, we apply the additional criterion that the telomere must contain unique affected genes, which may lead to an underestimation of the number of telomeres affected. According to these stringent criteria, affected telomeres in *yaf9*Δ strains are 2R, 3R, 4L, 4R, 6L, 11L 13R, 14R, and 15L (see Table S1 in the supplemental data), with several other telomeres being moderately affected. Affected telomeres do not appear to share an obvious common element (such as Y′) or attribute that would distinguish them clearly from other telomeres.

Our results show a striking overlap with telomeres affected in strains lacking Htz1 (see below and Table S1 in the supplemental data) (34). In keeping with the results and the focus of studies by others on Htz1 and Swr1, we chose to focus our detailed analysis on telomere 14R and the region between silent mating type locus *HMR* and telomere 3R (Fig. 5A). At telomere 14R, the loss of Yaf9 causes a significant downregulation of proximal genes (Fig. 5B). Likewise, several genes in the region between telomere 3R and *HMR* (YCR099C/100C/101C/104W) are affected (Fig. 5C and data not shown). Consistent with a role for NuA4 in this process, a mutation in the catalytic subunit of NuA4 that reduces H4 acetylation, *esa1-L254P* (8), confers significant downregulation of genes at 14R (Fig. 4A and 5B), although it has only a slight impact at 3R (data not shown). The impact of *esa1-L254P* on telomeres is

not as extensive as that observed with the *yaf9*Δ strain (see Table S1 in the supplemental data). However, we observed a significant overlap in the genes affected in *esa1-L254P* and *yaf9*Δ strains, and this overlap was quite pronounced when we considered the subset of affected genes located near telomeres (Fig. 5D).

In keeping with a role for Yaf9 in the SWR1 complex, about one-third of the genes downregulated in *htz1*Δ strains are identical to those downregulated in *yaf9*Δ strains (Fig. 5D). As with *esa1-L254P*, the overlap was even more extensive when we considered the subset of affected genes within 20 kb of the telomere; in that situation, the overlap approached 50%. Taken together, these results suggest that Yaf9 assists both SWR1/Htz1 and NuA4 complexes in telomere-proximal gene expression.

***sas5*Δ strains show extensive repression of telomere-proximal genes.** Strains lacking Sas2 show extensive downregulation of genes near certain telomeres, and their downregulation is correlated with a reduction in histone H4 acetylation (26, 49). However, the impact of the associated YEATS protein Sas5 on this process has not been determined. We found that a loss of Sas5 affects telomeres 1L, 2R, 3R, 4R, 5L, 6L, 7L, 9R,11L, 12R, 13R, 14R, 15L, and 16R (using the criteria established above), although many additional telomeres are moderately affected (see Table S1 in the supplemental data). The work of others on *sas2*Δ focused on selected telomeres, primarily 6R, which is one of the two telomeres for which gene(s) are lacking on our array and which therefore could not be analyzed. These results extend the importance of the YEATS family in the process of gene expression or antisilencing at telomeres in vivo. These results also suggest that certain telomeres, such as 14R, rely on multiple complexes for antisilencing, whereas others depend primarily on the SAS complex.

Loss of *SIR3* partially reverses *yaf9*Δ gene expression profiles and phenotypes. Downregulation of genes at telomere-proximal loci might be a consequence of the spreading of Sir3 into these regions, a reduction in histone H4 acetylation in these regions, a reduction in Htz1 replacement in these regions, or a combination of these factors. To help discern among these possibilities, we determined whether downregulated telomere-proximal genes acquire Sir3 and the extent to which their downregulation depends on Sir3. Interestingly, the removal of Sir3 from strains lacking Yaf9 restores the transcription (either partially or fully) of certain genes (*PAU6* and YNR074 for 14R; *GIT1* and YCR099C/100C for 3R), whereas the transcription of other loci in these regions is not restored. We suggest that genes whose transcription is restored by the removal of Sir3 are those silenced by the Sir complex (in *yaf9*Δ strains), whereas those that remain silent in the *yaf9*Δ *sir3*Δ double mutant are deficient in histone acetylation and/or Htz1 replacement due to the absence of Yaf9 (see below).

As the loss of *SIR3* partially restores the profiles of expression of telomere-proximal genes in *yaf9*Δ, the loss of *SIR3* might suppress certain *yaf9*Δ phenotypes. Compared to *yaf9*Δ mutants, *sir3*Δ *yaf9*Δ double mutants show slightly improved growth at low temperatures and WT growth on medium containing caffeine (Fig. 3D), suggesting that these defects in *yaf9*Δ strains are related to telomere-proximal gene repression caused by the spreading of Sir proteins. However, no suppression of phenotypes related to DNA repair and metabolism was observed, suggesting that these defects are not restricted to functions at telomeres and are not related to Sir protein spreading. These results further suggest that Yaf9, as a member of either the SWR1 complex or the NuA4 complex, plays roles both at telomeres and at other loci.

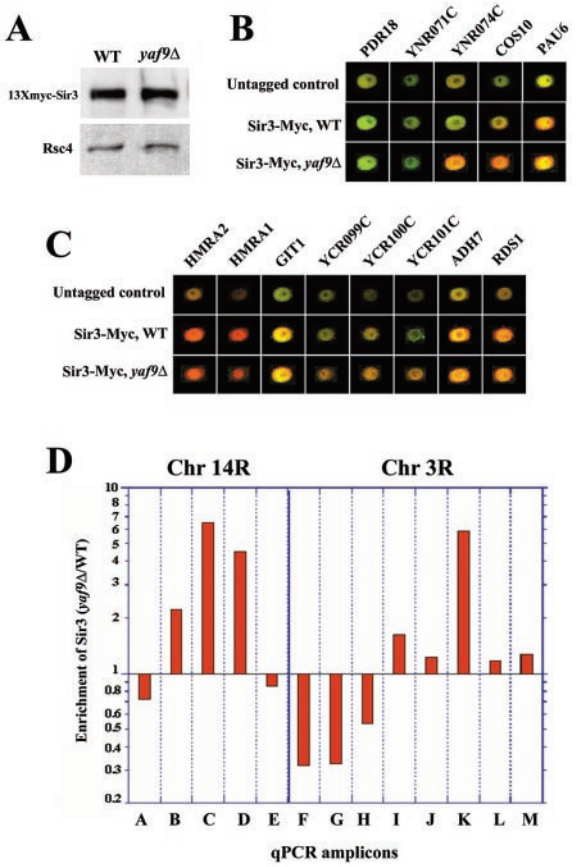

FIG. 6. Spreading of Sir3 in *yaf9*Δ strains. (A) Sir3-Myc levels are identical in WT and *yaf9*Δ strains, as shown by immunoblot analysis of whole-cell extracts derived from WT and *yaf9*Δ strains. (B) Sir3-Myc occupancy at telomere 14R in WT and *yaf9*Δ strains, as revealed by G-ChIP analysis. Input DNA was labeled with Cy3 (green) and DNA enriched by ChIP was labeled with Cy5 (red) and hybridized competitively to the genomic microarray. Cy5/Cy3 ratios were normalized as described in the supplemental data. Spots corresponding to loci at telomere 14R were culled from the array (from one experiment) and arranged according to the physical map. Similar enrichments were observed in three separate experiments. (C) As in panel B, but for telomere 3R. (D) Sir3 occupancy and spreading in the *yaf9*Δ strain at telomeres 3R and 14R, as revealed by qPCR. Figure 5A shows the physical locations of primer set amplicons. Values represent the enrichment of Sir3 in *yaf9*Δ cells divided by that in WT cells (see Materials and Methods). Values shown represent the median of three independent ChIP experiments with qPCR determinations performed twice (see the supplemental data). Chr, chromosome.

Silencing of telomere-proximal genes in *yaf9*Δ strains correlates with occupancy by Sir3. To directly determine the extent of Sir3 spreading in *yaf9*Δ strains, we performed ChIP of Sir3 in WT and *yaf9*Δ strains, each bearing a *SIR3* allele encoding a Myc_{13}-tagged Sir3 derivative integrated at the *SIR3* locus. The levels of Myc_{13}-tagged Sir3 protein were virtually identical in WT and *yaf9*Δ strains (Fig. 6A). We then assessed the enrichment of particular loci by two methods: (i) genome-

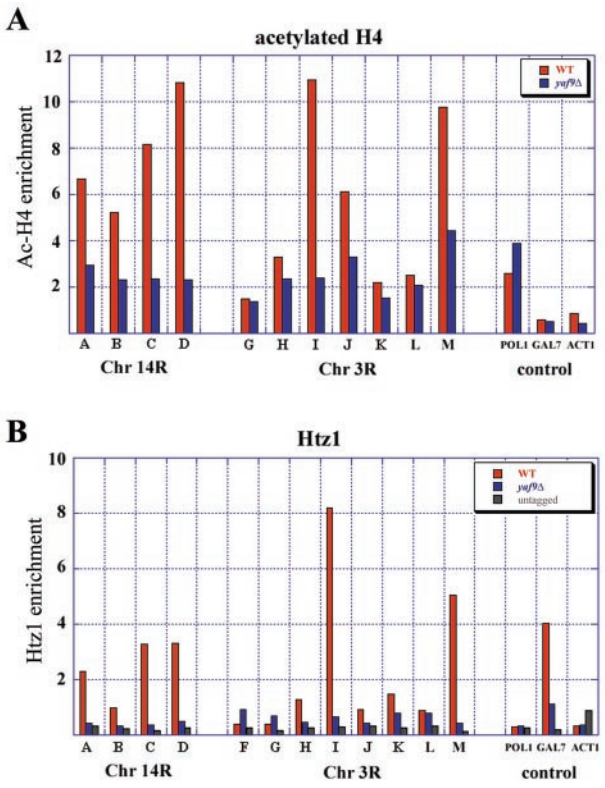

FIG. 7. Yaf9 is important for histone H4 acetylation and is essential for Htz1 deposition at telomeres 14R and 3R. Relative acetylated H4 (Ac-H4) enrichment (A) and Htz1 enrichment (B) for WT (red) and *yaf9*Δ (blue) strains are shown. Enrichment was quantified by qPCR. Figure 5A shows the physical locations of primer set amplicons. Values shown represent the median of three independent ChIP experiments with qPCR determinations performed twice. Chr, chromosome.

wide occupancy determinations involving ChIP combined with an immobilized array of the entire yeast genome parsed into open reading frame and intergenic fragments (G-ChIP) and (ii) qPCR. For telomere14R, telomere-proximal *PAU6* is highly occupied by Sir3 in both WT and *yaf9*Δ strains, as indicated by both G-ChIP (Fig. 6B) and qPCR (Fig. 6D). Note that Fig. 6D depicts the relative enrichment of Sir3 in the *yaf9*Δ strain compared to the WT strain, whereas the intensity of Cy5 (red) in the G-ChIP assay (Fig. 6B and C) reflects the absolute levels of Sir3. In the *yaf9*Δ strain, a redistribution of Sir3 is clearly observed at telomere 14R, consistent with spreading from the telomere end toward internal genes (Fig. 6B and D). Likewise, genes interposed between *HMR* and telomere 3R display increased Sir3 occupancy. Also, a reduction in occupancy at *HMR* itself was revealed by qPCR, suggesting that the spreading of Sir3 to the intervening region may come from (or at the expense of) *HMR*; however, a very significant amount of Sir3 remains (Fig. 6C and data not shown).

Loss of Yaf9 correlates with loss of H4 hyperacetylation at telomeres 14R and 3R. To test whether downregulation near telomeres is correlated with reductions in H4 acetylation, we performed ChIP analyses with an antibody raised against the hyperacetylated (at K5, K8, K12, and K16) tail of histone H4. For WT cells, we observed high levels of H4 acetylation at particular loci in both regions. Interestingly, these loci are either near or at the boundary of Sir3 spreading in WT cells (*COS10* for 14R and *GIT1* and *RDS1* for 3R) (Fig. 7A). However, *RDS1* is both occupied by Sir3 and significantly acetylated, suggesting that H4 acetylation may not entirely prevent Sir3 binding or that the region is dynamic with respect to acetylation and deacetylation or Sir binding. For *yaf9*Δ cells, we observed a significant reduction in the acetylation of these loci but not of several other control loci. However, as similar reductions at these loci have been observed in strains lacking Htz1 (34), we cannot directly attribute the entire effect to Yaf9 assisting acetylation by NuA4 (see Discussion).

Htz1 occupancy at telomeres is reduced significantly in *yaf9*Δ strains. Our genetic and genomic results all suggest a close functional connection between Yaf9 and Htz1, raising the possibility that Yaf9 may assist the SWR1 complex in the deposition of Htz1 in vivo. To test this possibility, we used ChIP and qPCR to assess the occupancy of Htz1 in WT and *yaf9*Δ strains. To this end, we deleted *YAF9* from a strain bearing an *HTZ1* allele encoding an HA_3-tagged version of Htz1 integrated at its genomic locus. Initially, we performed ChIP for both strains and quantified the enrichment of loci at telomeres 14R and 3R by qPCR. As observed with our H4 ChIP analyses, only certain loci are occupied by Htz1. Interestingly, although the sample size is small, there appears to be a significant correlation between loci showing H4 hyperacetylation and loci showing Htz1 occupancy, raising the possibility that these two functions are linked. Remarkably, Htz1 occupancy is significantly reduced at the telomeric loci tested in the *yaf9*Δ strain (Fig. 7B). Interestingly, the reduction in Htz1 occupancy in the *yaf9*Δ strain may not be restricted to telomeres, as Htz1 occupancy is also reduced at *GAL7*.

To determine whether deletion of *YAF9* affected the assembly of the SWR1 complex, we performed gel filtration analyses with WT and *yaf9*Δ strains bearing a Myc-tagged Swr1 derivative. For both strains, the SWR1 complex eluted at a molecular mass of 700 to 850 kDa (data not shown), suggesting that the complex remains intact in the *yaf9*Δ strain.

DISCUSSION

Chromosomes contain regions of specialized chromatin to help regulate chromosomal processes and transcriptional programs. For example, centromeres and telomeres represent loci where special chromatin structures are initiated to assist in processes such as kinetochore formation, sister chromatid cohesion, and DNA end protection and replication processes (for telomeres). RNA polymerase II transcription in these regions may interfere with the fidelity of these processes; this activity likely underlies the paucity of polymerase II genes in these regions. The heterochromatin of telomeres includes Sir proteins, which have the capacity to silence telomere-proximal genes via histone deacetylation. As Sir proteins bind to deacetylated histone tails, cycles of deacetylation and binding allow the Sir complex to spread and polymerize down the chromatin, extending silencing to neighboring regions. However, the spreading process must be limited (or regulated) to avoid improper silencing of neighboring polymerase II genes. This work provides evidence that YEATS family transcription factors help limit the propagation of silent heterochromatin

through their functions in histone modifying and remodeling complexes.

YEATS proteins as members of chromatin and transcription complexes. YEATS proteins were originally discovered through the cloning of reciprocal chromosomal translocations involving the MLL/HRX/ALL-1 gene. These translocations encoded MLL-YEATS fusion proteins, which are commonly found in acute leukemias. Studies with yeast cells have firmly connected the YEATS protein family to transcription and chromatin (see the introduction). Here we show that the YEATS protein family in yeast cells (overall) is essential for viability and provide evidence that the YEATS domain itself is important for function, as mutations in conserved residues in the domain confer significant phenotypes. At present, we are not able to determine whether these substitutions eliminate YEATS domain function entirely or just impair it significantly; therefore, it remains possible that the YEATS domain is required for all functions of Yaf9 and Taf14. As a YEATS family member is present in all three currently identified chromatin remodeling and modifying complexes involved in telomere-proximal gene expression (SAS/NuA4/SWR1), identification of the binding partner for the YEATS domain may reveal a unifying role.

Recent work strongly suggests that the human TIP60 complex is the human counterpart of the yeast NuA4 complex, as they contain 11 paralogous subunits (5, 12, 13). The TIP60 complex contains the YEATS protein Gas41, and the yeast protein most similar to Gas41 is Yaf9 (Fig. 1) (32). Our data show further that the Yaf9 C terminus is required for the assembly of Yaf9 into NuA4. This result is interesting in light of the critical role of the C terminus in MLL fusions involving YEATS proteins; the C terminus is a constant feature of all leukemogenic fusions, whereas the YEATS domain can be absent. Current models suggest that the MLL amino terminus present in fusion proteins retains the domains important for targeting to HOX genes. We suggest that the C terminus of the YEATS partner may represent a domain for an HAT-remodeler interaction that enables the misregulation of HOX genes by improper HAT-remodeler recruitment.

Histone acetylation in boundary formation. Recent data from several laboratories indicates the coordinated efforts of HATs, remodelers, and Htz1 in opposing the spreading of Sir proteins at yeast telomeres (see the introduction). For the acetylation component, H4 acetylation appears to be key, although there is also evidence that H3 acetylation plays a role at certain telomeres (28). Clearly, the factor with the most significant impact at telomeres is the SAS complex (26, 49), based on the large spectrum of telomeres involved (see Table S1 in the supplemental data). The SAS complex (Sas2/4/5) consists of the MYST family HAT Sas2p, Sas4, and the YEATS protein Sas5 (33, 40). Sas2 has a clear preference for H4K16 in vitro, and cells lacking Sas2 show a significant reduction in H4K16 acetylation (33, 49). Earlier studies established the concept that H4K16 acetylation by Sas2 at telomeres is important for limiting Sir spreading (26, 49) and focused on the role of Sas2 and its impact at chromosome 6R. Here, our transcription profiling of *sas5*Δ strains revealed a significant impact on silencing at the vast majority of yeast telomeres (see Table S1 in the supplemental data). This result is consistent with the observations that the SAS complex lacking Sas5 shows reduced HAT activity in vitro and that *sas5* mutations affect silencing at *HMR* (51, 53). Taken together, these studies establish an important role for the YEATS protein Sas5 in assisting the SAS complex at yeast telomeres.

A *yaf9*Δ mutation has a clear effect on telomere-proximal gene expression. However, as Yaf9 is present in both SWR1 and NuA4, it is difficult to attribute Yaf9 functions to a particular complex. To help clarify its role in NuA4, we examined the role of histone acetylation by Esa1. A role for Esa1 in promoting gene expression at genes near telomere 6R had been demonstrated previously (49), whereas we assessed the impact of an *esa1* mutation genome-wide and observed down-regulation at several telomeres, revealing a fairly broad role for Esa1. Importantly, we found a significant overlap in the genes affected near telomeres in *esa1-L254P* and *yaf9*Δ strains (Fig. 5D). However, as the *esa1-L254P* allele is still partially functional, the full impact of Esa1 on telomere-proximal gene expression (and its overlap in function with Yaf9) may be significantly greater than was observed with *esa1-L254P*. Furthermore, we show that H4 acetylation is reduced at affected telomeres in *yaf9*Δ strains. Although this result is consistent with Yaf9 assisting NuA4 in acetylation at these loci, reductions at these loci are also observed in strains lacking Htz1 (34). Thus, the reductions in H4 acetylation observed in *yaf9*Δ strains may be due to a combination of reduced NuA4 function, increased Sir2/3/4 (histone deacetylase) spreading, and the lack of Htz1 at these loci.

Studies of Esa1 specificity in vitro and in vivo strongly suggest that Esa1 (also a MYST family HAT) contributes the majority of acetylation at H4K5/8/12 and a portion of the acetylation at H4K16 (2, 46, 49). Thus, together, Sas2 and Esa1 constitute the majority of H4 acetyltransferase activity in yeast cells, and it seems reasonable to propose that these two HATs work together to regulate H4 acetylation at telomeres. Furthermore, their different specificities raise the possibility that acetylation by one HAT may improve acetylation by the other HAT. Support for these proposals was revealed in the acetylation profile of *sas2 esa1* double mutants at 6R, which showed greater-than-additive reductions in H4K16 acetylation near telomeres than either single mutant (49). As both the SAS complex and the NuA4 complex contain YEATS proteins, it is tempting to speculate that YEATS proteins may assist in the targeting of these complexes to telomeres through the recognition of an aspect of telomeric chromatin, such as Htz1.

Histone replacement in boundary formation. Important roles for Htz1 in boundary formation and SWR1 in Htz1 replacement were recently established, but much about the regulation of this process is not understood (see Introduction). Here we provide several lines of evidence that Yaf9 contributes to the Htz1 deposition process. First, *yaf9*Δ strains and *htz1*Δ strains show significant overlap in phenotypes. However, their phenotypes are not identical (*yaf9*Δ strains are more sensitive to MMS, for example), suggesting that Yaf9 has roles beyond those attributed to SWR1. These roles likely involve the functions of Yaf9 in NuA4, as it is a stable member of NuA4 and as NuA4 mutants are likewise very sensitive to DNA-damaging agents such as MMS. Second, *yaf9*Δ strains and *htz1*Δ strains show significant overlap in both affected genes and affected telomeres. Third, *yaf9*Δ strains show dramatic reductions in Htz1 deposition at telomeres. Taken to-

gether, these data indicate that Yaf9 plays a functional role in the SWR1 complex in Htz1 deposition. Several important questions remain, including how the SWR1 complex is targeted to particular loci, how the process of replacement is regulated by complex members, and how Htz1 replacement and H4 acetylation are linked.

Combining histone acetylation, histone replacement, and transcriptional activity to establish and maintain boundaries. Emerging evidence strongly suggests that antisilencing at telomeres requires the coordinated functions of HATs, remodelers, and a histone variant. However, several central issues remain. For example, it is not clear why spreading is observed at certain telomeres and not others as a consequence of the loss of certain HAT or SWR1 components. One might expect that the strength of the barrier at a particular telomere would correlate with the rates of transcription of resident genes. Indeed, a strongly transcribed ribosomal protein gene or the isolated promoters of highly transcribed genes can limit Sir propagation in certain contexts (4, 54). Also, tRNAs can serve as effective barriers to propagation (10, 11), although they are not uniformly present near telomere ends and the generality of their use as barriers has not been established. However, transcription itself is not required for Reb1 and Tbf1 to serve as barriers at subtelomeric X elements (15), and an examination of native boundaries and transcriptional activity has not been thoroughly performed. Thus, the relationship between transcription and barrier formation at native telomeres is still emerging and requires further work. Another interesting question is the order in which the processes occur, e.g., whether histone acetylation serves as a mark for Htz1 replacement or whether nucleosomes that bear Htz1 are themselves preferred substrates for SAS or NuA4 complexes. Either scenario would provide an effective combination of these processes to establish and or maintain boundaries.

Biology of telomere-proximal silencing. The phenomenon of gene silencing near telomeres has revealed many interesting silencing proteins as well as important concepts in epigenetics. However, the context in which a yeast cell may utilize a position effect to increase fitness has only recently come to light. Studies by Ai and colleagues recently showed that stress conditions lead to the activation of Mpk1/Slt2 kinase and the phosphorylation of Sir3, which leads to a reduction in Sir3 occupancy of genes near telomeres (1). Remarkably, many genes that participate in the response to stress involving the cell wall are telomere proximal, leading to their expression under cell wall stress conditions. Therefore, in this context, the telomere may consist of two distinct regions: (i) subtelomeric regions with few or no genes, as transcription may interfere with DNA end protection and replication processes, and (ii) telomere-proximal regions bearing polymerase II genes that utilize the dynamic properties of the spreading process to control their expression programs via position effects. Clearly, understanding how HATs and SWR1/Htz1 function to control spreading dynamics will be central to understanding the regulation of these gene programs.

ACKNOWLEDGMENTS

We thank Brian Dalley and Adrienne Tew from the HCI microarray core facility for assistance. We thank Bob Schackmann for oligonucleotide synthesis and Mitch Smith for strain HA-HTZ1.

This work was supported by National Institutes of Health grants 5-T32DK07115-29 (to J. Kushner, for support of D. N. Roberts and D. O. Richardson), GM60415 (to B. R. Cairns, for support of H. Zhang), and CA24014 (for core facilities). J.C. is an investigator with the Canadian Institutes of Health Research. This work was also supported by the Howard Hughes Medical Institute (HHMI). B.R.C. is an investigator with the Huntsman Cancer Institute and an assistant investigator with HHMI.

REFERENCES

1. **Ai, W., P. G. Bertram, C. K. Tsang, T. F. Chan, and X. F. Zheng.** 2002. Regulation of subtelomeric silencing during stress response. Mol. Cell **10:** 1295–1305.
2. **Allard, S., R. T. Utley, J. Savard, A. Clarke, P. Grant, C. J. Brandl, L. Pillus, J. L. Workman, and J. Cote.** 1999. NuA4, an essential transcription adaptor/histone H4 acetyltransferase complex containing Esa1p and the ATM-related cofactor Tra1p. EMBO J. **18:**5108–5119.
3. **Angus-Hill, M. L., A. Schlichter, D. Roberts, H. Erdjument-Bromage, P. Tempst, and B. R. Cairns.** 2001. A Rsc3/Rsc30 zinc cluster dimer reveals novel roles for the chromatin remodeler RSC in gene expression and cell cycle control. Mol. Cell **7:**741–751.
4. **Bi, X., and J. R. Broach.** 1999. UASrpg can function as a heterochromatin boundary element in yeast. Genes Dev. **13:**1089–1101.
5. **Cai, Y., J. Jin, C. Tomomori-Sato, S. Sato, I. Sorokina, T. J. Parmely, R. C. Conaway, and J. W. Conaway.** 2003. Identification of new subunits of the multiprotein mammalian TRRAP/TIP60-containing histone acetyltransferase complex. J. Biol. Chem. **278:**42733–42736.
6. **Cairns, B. R., N. L. Henry, and R. D. Kornberg.** 1996. TFG/TAF30/ANC1, a component of the yeast SWI/SNF complex that is similar to the leukemogenic proteins ENL and AF-9. Mol. Cell. Biol. **16:**3308–3316.
7. **Carmen, A. A., L. Milne, and M. Grunstein.** 2002. Acetylation of the yeast histone H4 N terminus regulates its binding to heterochromatin protein SIR3. J. Biol. Chem. **277:**4778–4781.
8. **Clarke, A. S., J. E. Lowell, S. J. Jacobson, and L. Pillus.** 1999. Esa1p is an essential histone acetyltransferase required for cell cycle progression. Mol. Cell. Biol. **19:**2515–2526.
9. **Dhillon, N., and R. T. Kamakaka.** 2000. A histone variant, Htz1p, and a Sir1p-like protein, Esc2p, mediate silencing at HMR. Mol. Cell **6:**769–780.
10. **Donze, D., C. R. Adams, J. Rine, and R. T. Kamakaka.** 1999. The boundaries of the silenced HMR domain in Saccharomyces cerevisiae. Genes Dev. **13:**698–708.
11. **Donze, D., and R. T. Kamakaka.** 2001. RNA polymerase III and RNA polymerase II promoter complexes are heterochromatin barriers in Saccharomyces cerevisiae. EMBO J. **20:**520–531.
12. **Doyon, Y., and J. Cote.** 2004. The highly conserved and multifunctional NuA4 HAT complex. Curr. Opin. Genet. Dev. **14:**147–154.
13. **Doyon, Y., W. Selleck, W. S. Lane, S. Tan, and J. Cote.** 2004. Structural and functional conservation of the NuA4 histone acetyltransferase complex from yeast to humans. Mol. Cell. Biol. **24:**1884–1896.
14. **Eisen, A., R. T. Utley, A. Nourani, S. Allard, P. Schmidt, W. S. Lane, J. C. Lucchesi, and J. Cote.** 2001. The yeast NuA4 and Drosophila MSL complexes contain homologous subunits important for transcription regulation. J. Biol. Chem. **276:**3484–3491.
15. **Fourel, G., C. Boscheron, E. Revardel, E. Lebrun, Y. F. Hu, K. C. Simmen, K. Muller, R. Li, N. Mermod, and E. Gilson.** 2001. An activation-independent role of transcription factors in insulator function. EMBO Rep. **2:**124–132.
16. **Fourel, G., T. Miyake, P. A. Defossez, R. Li, and E. Gilson.** 2002. General regulatory factors (GRFs) as genome partitioners. J. Biol. Chem. **277:**41736–41743.
17. **Fourel, G., E. Revardel, C. E. Koering, and E. Gilson.** 1999. Cohabitation of insulators and silencing elements in yeast subtelomeric regions. EMBO J. **18:**2522–2537.
18. **Galarneau, L., A. Nourani, A. A. Boudreault, Y. Zhang, L. Heliot, S. Allard, J. Savard, W. S. Lane, D. J. Stillman, and J. Cote.** 2000. Multiple links between the NuA4 histone acetyltransferase complex and epigenetic control of transcription. Mol. Cell **5:**927–937.
19. **Grunstein, M.** 1997. Molecular model for telomeric heterochromatin in yeast. Curr. Opin. Cell Biol. **9:**383–387.
20. **Hecht, A., S. Strahl-Bolsinger, and M. Grunstein.** 1996. Spreading of transcriptional repressor SIR3 from telomeric heterochromatin. Nature **383:**92–96.
21. **Henry, N. L., A. M. Campbell, W. J. Feaver, D. Poon, P. A. Weil, and R. D. Kornberg.** 1994. TFIIF-TAF-RNA polymerase II connection. Genes Dev. **8:**2868–2878.
22. **Ikura, T., V. V. Ogryzko, M. Grigoriev, R. Groisman, J. Wang, M. Horikoshi, R. Scully, J. Qin, and Y. Nakatani.** 2000. Involvement of the TIP60 histone acetylase complex in DNA repair and apoptosis. Cell **102:**463–473.
23. **Imai, S., C. M. Armstrong, M. Kaeberlein, and L. Guarente.** 2000. Transcriptional silencing and longevity protein Sir2 is an NAD-dependent histone deacetylase. Nature **403:**795–800.

24. **Jenuwein, T., and C. D. Allis.** 2001. Translating the histone code. Science **293:**1074–1080.
25. **John, S., L. Howe, S. T. Tafrov, P. A. Grant, R. Sternglanz, and J. L. Workman.** 2000. The something about silencing protein, Sas3, is the catalytic subunit of NuA3, a yTAF(II)30-containing HAT complex that interacts with the Spt16 subunit of the yeast CP (Cdc68/Pob3)-FACT complex. Genes Dev. **14:**1196–1208.
26. **Kimura, A., T. Umehara, and M. Horikoshi.** 2002. Chromosomal gradient of histone acetylation established by Sas2p and Sir2p functions as a shield against gene silencing. Nat. Genet. **32:**370–377.
27. **Kobor, M. S., S. Venkatasubrahmanyam, M. D. Meneghini, J. W. Gin, J. L. Jennings, A. J. Link, H. D. Madhani, and J. Rine.** 2004. A protein complex containing the conserved Swi2/Snf2-related ATPase Swr1p deposits histone variant H2A.Z into euchromatin. PLoS Biol. **2:**587–599.
28. **Kristjuhan, A., B. O. Wittschieben, J. Walker, D. Roberts, B. R. Cairns, and J. Q. Svejstrup.** 2003. Spreading of Sir3 protein in cells with severe histone H3 hypoacetylation. Proc. Natl. Acad. Sci. USA **100:**7551–7556.
29. **Krogan, N. J., M. C. Keogh, N. Datta, C. Sawa, O. W. Ryan, H. Ding, R. A. Haw, J. Pootoolal, A. Tong, V. Canadien, D. P. Richards, X. Wu, A. Emili, T. R. Hughes, S. Buratowski, and J. F. Greenblatt.** 2003. A Snf2 family ATPase complex required for recruitment of the histone H2A variant Htz1. Mol. Cell **12:**1565–1576.
30. **Ladurner, A. G., C. Inouye, R. Jain, and R. Tjian.** 2003. Bromodomains mediate an acetyl-histone encoded antisilencing function at heterochromatin boundaries. Mol. Cell **11:**365–376.
31. **Landry, J., A. Sutton, S. T. Tafrov, R. C. Heller, J. Stebbins, L. Pillus, and R. Sternglanz.** 2000. The silencing protein SIR2 and its homologs are NAD-dependent protein deacetylases. Proc. Natl. Acad. Sci. USA **97:**5807–5811.
32. **Le Masson, I., D. Y. Yu, K. Jensen, A. Chevalier, R. Courbeyrette, Y. Boulard, M. M. Smith, and C. Mann.** 2003. Yaf9, a novel NuA4 histone acetyltransferase subunit, is required for the cellular response to spindle stress in yeast. Mol. Cell. Biol. **23:**6086–6102.
33. **Meijsing, S. H., and A. E. Ehrenhofer-Murray.** 2001. The silencing complex SAS-I links histone acetylation to the assembly of repressed chromatin by CAF-I and Asf1 in Saccharomyces cerevisiae. Genes Dev. **15:**3169–3182.
34. **Meneghini, M. D., M. Wu, and H. D. Madhani.** 2003. Conserved histone variant H2A.Z protects euchromatin from the ectopic spread of silent heterochromatin. Cell **112:**725–736.
35. **Mizuguchi, G., X. Shen, J. Landry, W. H. Wu, S. Sen, and C. Wu.** 2004. ATP-driven exchange of histone H2AZ variant catalyzed by SWR1 chromatin remodeling complex. Science **303:**343–348.
36. **Mumberg, D., R. Muller, and M. Funk.** 1994. Regulatable promoters of Saccharomyces cerevisiae: comparison of transcriptional activity and their use for heterologous expression. Nucleic Acids Res. **22:**5767–5768.
37. **Nakamura, T., H. Alder, Y. Gu, R. Prasad, O. Canaani, N. Kamada, R. P. Gale, B. Lange, W. M. Crist, P. C. Nowell, et al.** 1993. Genes on chromosomes 4, 9, and 19 involved in 11q23 abnormalities in acute leukemia share sequence homology and/or common motifs. Proc. Natl. Acad. Sci. USA **90**:4631–4635.
38. **Nourani, A., R. T. Utley, S. Allard, and J. Cote.** 2004. Recruitment of the NuA4 complex poises the PHO5 promoter for chromatin remodeling and activation. EMBO J. **23:**2597–2607.
39. **Oki, M., L. Valenzuela, T. Chiba, T. Ito, and R. T. Kamakaka.** 2004. Barrier proteins remodel and modify chromatin to restrict silenced domains. Mol. Cell. Biol. **24:**1956–1967.
40. **Osada, S., A. Sutton, N. Muster, C. E. Brown, J. R. Yates III, R. Sternglanz, and J. L. Workman.** 2001. The yeast SAS (something about silencing) protein complex contains a MYST-type putative acetyltransferase and functions with chromatin assembly factor ASF1. Genes Dev. **15:**3155–3168.
41. **Poon, D., Y. Bai, A. M. Campbell, S. Bjorklund, Y. J. Kim, S. Zhou, R. D. Kornberg, and P. A. Weil.** 1995. Identification and characterization of a TFIID-like multiprotein complex from Saccharomyces cerevisiae. Proc. Natl. Acad. Sci. USA **92:**8224–8228.
42. **Puig, O., F. Caspary, G. Rigaut, B. Rutz, E. Bouveret, E. Bragado-Nilsson, M. Wilm, and B. Seraphin.** 2001. The tandem affinity purification (TAP) method: a general procedure of protein complex purification. Methods **24:** 218–229.
43. **Reid, J. L., V. R. Iyer, P. O. Brown, and K. Struhl.** 2000. Coordinate regulation of yeast ribosomal protein genes is associated with targeted recruitment of Esa1 histone acetylase. Mol. Cell **6:**1297–1307.
44. **Roberts, D. N., A. J. Stewart, J. T. Huff, and B. R. Cairns.** 2003. The RNA polymerase III transcriptome revealed by genome-wide localization and activity-occupancy relationships. Proc. Natl. Acad. Sci. USA **100:**14695–14700.
45. **Sayre, M. H., H. Tschochner, and R. D. Kornberg.** 1992. Reconstitution of transcription with five purified initiation factors and RNA polymerase II from Saccharomyces cerevisiae. J. Biol. Chem. **267:**23376–23382.
46. **Smith, E. R., A. Eisen, W. Gu, M. Sattah, A. Pannuti, J. Zhou, R. G. Cook, J. C. Lucchesi, and C. D. Allis.** 1998. ESA1 is a histone acetyltransferase that is essential for growth in yeast. Proc. Natl. Acad. Sci. USA **95:**3561–3565.
47. **Smith, J. S., C. B. Brachmann, I. Celic, M. A. Kenna, S. Muhammad, V. J. Starai, J. L. Avalos, J. C. Escalante-Semerena, C. Grubmeyer, C. Wolberger, and J. D. Boeke.** 2000. A phylogenetically conserved NAD+-dependent protein deacetylase activity in the Sir2 protein family. Proc. Natl. Acad. Sci. USA **97:**6658–6663.
48. **Strahl-Bolsinger, S., A. Hecht, K. Luo, and M. Grunstein.** 1997. SIR2 and SIR4 interactions differ in core and extended telomeric heterochromatin in yeast. Genes Dev. **11:**83–93.
49. **Suka, N., K. Luo, and M. Grunstein.** 2002. Sir2p and Sas2p opposingly regulate acetylation of yeast histone H4 lysine16 and spreading of heterochromatin. Nat. Genet. **32:**378–383.
50. **Suka, N., Y. Suka, A. A. Carmen, J. Wu, and M. Grunstein.** 2001. Highly specific antibodies determine histone acetylation site usage in yeast heterochromatin and euchromatin. Mol. Cell **8:**473–479.
51. **Sutton, A., W. J. Shia, D. Band, P. D. Kaufman, S. Osada, J. L. Workman, and R. Sternglanz.** 2003. Sas4 and Sas5 are required for the histone acetyltransferase activity of Sas2 in the SAS complex. J. Biol. Chem. **278:**16887–16892.
52. **Tkachuk, D. C., S. Kohler, and M. L. Cleary.** 1992. Involvement of a homolog of Drosophila trithorax by 11q23 chromosomal translocations in acute leukemias. Cell **71:**691–700.
53. **Xu, E. Y., S. Kim, and D. H. Rivier.** 1999. SAS4 and SAS5 are locus-specific regulators of silencing in Saccharomyces cerevisiae. Genetics **153:**25–33.
54. **Yu, Q., R. Qiu, T. B. Foland, D. Griesen, C. S. Galloway, Y. H. Chiu, J. Sandmeier, J. R. Broach, and X. Bi.** 2003. Rap1p and other transcriptional regulators can function in defining distinct domains of gene expression. Nucleic Acids Res. **31:**1224–1233.